RESEARCH ARTICLE
ONCOLOGY

Diseases & Research

Evaluating the Boron Neutron Capture Therapeutic Threshold of Boron-Containing Carbon Dots in Diverse Tumor Cell Lines

Haoyang Hao[1,*], Zhijie Wang[1,*], Mingxin Yang[1,2], Bingbing Peng[1], Shaokai Bai[1], Weihong Gu[3,#], Weihua Zhang[4,#], Gengmei Xing[1,#], Juan Li[1,#]

[1] Laboratory for Biomedical Effects of Nanomaterial and Nanosafety, Institute of High Energy Physics, Chinese Academy of Sciences, Beijing 100049, China
[2] University of Chinese Academy of Sciences, Beijing 100049, China
[3] CSPC ZhongQi Pharmaceutical Technology (Shijiazhuang) Company, Ltd , Shijiazhuang 050000, China
[4] Tsinghua University, Haidian District, Beijing 100084, China

Backgrounds: Boron neutron capture therapy (BNCT) is a binary precision radiotherapy that selectively kills tumor cells via high-linear energy transfer α-particles from the ^{10}B-neutron capture reaction, while preserving healthy tissues. Its efficacy is fundamentally limited by intracellular boron delivery efficiency. Boron-containing carbon dots (BCDs) are promising delivery agents with excellent biocompatibility, but systematic studies on their BNCT performance across diverse tumor types remain insufficient.
Methods: We evaluated BCDs in four tumor cell lines: U87-MG (glioblastoma), 4T-1 (breast cancer), HepG-2 (hepatocellular carcinoma), and B16-F10 (melanoma). We assessed dose-dependent cellular boron uptake via ICP-MS, cytotoxicity after thermal neutron irradiation *via* CCK-8 assay, and absorbed dose *via* Monte Carlo PHITS simulation, with statistical analysis by one-way ANOVA and Tukey's post-hoc test.
Results: BCDs showed concentration-dependent internalization with significant heterogeneous uptake across cell lines. U87-MG and 4T-1 had superior boron uptake and high BNCT sensitivity, while HepG-2 exhibited marked resistance (43-fold lower uptake than U87-MG), and B16-F10 showed moderate uptake. A critical therapeutic threshold was identified: significant cell killing only occurred when intracellular boron exceeded 20 μg [B]/mL with sufficient neutron fluence.
Conclusion: This study reveals the heterogeneous metabolic profiles of BCDs across different cancer types, and validates BCDs as a broad-spectrum radiosensitizing nanoplatform for BNCT. The identified critical intracellular boron therapeutic threshold provides a key reference for personalized dosimetry design and clinical translation of BCD-mediated BNCT.
Keywords: Boron neutron capture therapy; Boron-containing carbon dots; Cellular uptake; Therapeutic threshold; Nanomedicine; Radiation oncology.

Introduction

Boron neutron capture therapy (BNCT) presents a paradigm shift in precision radiotherapy, offering a binary approach to selectively target malignant cells while sparing adjacent healthy tissue[1–5]. The therapeutic mechanism hinges on the nuclear capture reaction between non-radioactive boron-10 (^{10}B) and low-energy thermal neutrons, producing high-linear energy transfer (LET) alpha particles (^{4}He) and recoiling lithium-7 (^{7}Li) nuclei[6–10]. Because the destructive range of these particles (<10 μm) is confined approximately to the diameter of a single cell, the success of BNCT is fundamentally dependent on achieving a critical concentration of ^{10}B specifically within tumor cells prior to neutron irradiation[11–13].

There are three essential elements of BNCT: First, the synthesis of ^{10}B compounds with high cancer cell affinity[14–16]. Second, due to the limited penetration of neutrons in living organisms, it is necessary to find a suitable type of cancer to be treated with this therapy[17–19]. Third, there must be a nuclear reactor or accelerator based neutron source with sufficient power to serve as a source of neutron rays[20–22]. Choosing the appropriate ^{10}B drug in BNCT treatment and delivering a sufficient amount of ^{10}B drug to tumor cells is the key to successful treatment[23–26].

The primary challenge impeding wider clinical application of BNCT remains the development of delivery agents that can achieve high tumor-to-normal tissue ratios and sufficient intracellular accumulation[8,27–30]. Recently, Boron-containing carbon dots (BCDs) have emerged as an innovative nanomedicine platform due to their ultrasmall size, excellent biocompatibility, fluorescence properties for tracking, and ability to penetrate biological barriers, including the blood-brain barrier[7,31–33].

As a potential boron carrier agent, the application research of

* These authors contributed equally to this work.
# Correspondence: Juan Li. E-mail: lijuan@ihep.ac.cn; Gengmei Xing. E-mail: xinggm@ihep.ac.cn. Address: Laboratory for Biomedical Effects of Nanomaterial and Nanosafety, Institute of High Energy Physics, Chinese Academy of Sciences, Beijing 100049, China; Weihua Zhang. E-mail: zwh110@tsinghua.edu.cn. Address: Tsinghua University, Haidian District, Beijing 100084, China; Weihong Gu. Email: 867361603@qq.com. Address: CSPC ZhongQi Pharmaceutical Technology (Shijiazhuang) Company, Ltd., Shijiazhuang 050000, China.
Received 20 December 2025; Revised 14 January 2026; Accepted 9 March 2026; Available Online 1 April 2026
DOI: 10.54457/DR.202601009

BCDs in BNCT still lacks sufficient studies, especially regarding the therapeutic responses in different tumor types. Previous studies have demonstrated the potential of BCDs in specific models, such as glioma (U87-MG)[3,31,32]. However, cancer is a heterogeneous disease, and the metabolic fate of nanomaterials varies significantly across different tumor origins (Fig. 1). To validate BCDs as a broad-spectrum BNCT vector, it is crucial to move beyond single-disease models and establish baseline metabolic profiles. This study aims to bridge this gap by conducting a comparative analysis of the metabolic dynamics and therapeutic efficacy of BCDs across distinct solid tumor cell lines, including glioblastoma (U87-MG)[34], breast cancer (4T-1), and hepatocellular carcinoma (HepG-2). By correlating intracellular boron uptake with cytotoxicity under varying neutron fluences, we seek to elucidate the factors governing tumor sensitivity to BCD-mediated BNCT and identify critical therapeutic concentration thresholds.

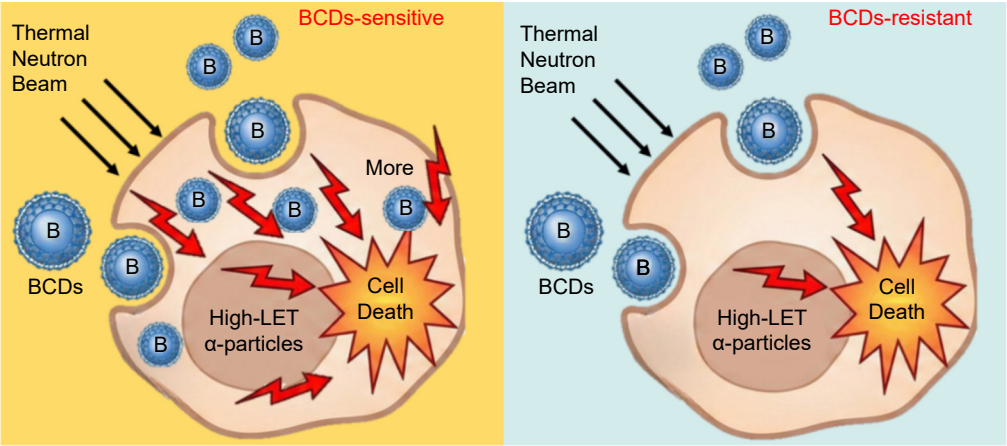

Fig. 1. The metabolic divergence segments the cell lines into "BCDs-sensitive" and "BCDs-resistant" populations with different BNCT treatment response.

Materials and Methods

Materials

Materials and Cell Lines Boron-containing carbon dots (BCDs) were synthesized and purified according to previously published protocols established in our laboratory[22]. The following tumor cell lines were obtained from the Peking Union Medical College Cell Bank: U87-MG (human glioblastoma), 4T-1 (murine breast cancer), HepG-2 (human hepatocellular carcinoma), and B16-F10 (murine melanoma). Cells were cultured in DMEM or RPMI-1640 medium supplemented with 10% fetal bovine serum (Gibco) and maintained in a humidified incubator at 37 °C with 5% CO_2.

Cellular Uptake Analysis

To evaluate internalization efficiency, cell suspensions (10^5 cells/mL) were seeded in 96-well plates (100 μL/well). Cells were incubated with varying concentrations of BCDs (0, 10, 20, 30, 50, 100 and 200 μg B/mL) for designated time intervals (8, 12, and 24 h). Following incubation, cells were washed thoroughly with PBS to remove non-internalized BCDs. The intracellular boron content was quantified using Inductively Coupled Plasma Mass Spectrometry (ICP-MS). The 50 μg B/mL concentration was selected for key experiments because it meets the minimum boron concentration threshold (20 μg B/mL) for all tested cell lines: B16-F10 cells reach sufficient intracellular boron levels at 50 μg B/mL, while U87-MG and 4T-1 cells exceed the threshold even at lower concentrations (35 ppm and 25 ppm respectively at 100 μg B/mL external concentration).

In Vitro BNCT Irradiation Experiments

For BNCT efficacy studies, cells were incubated with BCDs at specified concentrations to allow for uptake. Subsequently, the cells were exposed to thermal neutron irradiation at the China Spallation Neutron Source (CSNS, Guangdong). The irradiation parameters were set to achieve the targeted neutron fluence based on the facility's specifications (thermal neutron flux approx. 10^7–10^8 n/cm^2).

Cell Viability Assay

Following neutron irradiation, the medium was replaced with fresh medium containing 10% Cell Counting Kit-8 (CCK-8, Beiren Chemical Technology). Cells were incubated for an additional 4 hours. The optical density (OD) was measured at 490 nm using a microplate reader. Cell viability was calculated using the following formula:

$$\text{Cell Viability (\%)} = \left(\frac{OD_{sample} - OD_{blank}}{OD_{control} - OD_{blank}} \right) \times 100$$

Where: OD_{sample} is the optical density of the wells with treated cells (incubated with boron-containing carbon dots). $OD_{control}$ represents untreated cells, OD_{blank} represents media containing CCK-8 without cells.

Dosimetry Simulations

Micro-metrological analysis of the absorbed dose during BNCT was simulated using the Monte Carlo code PHITS (Particle and Heavy Ion Transport code System), following established protocols[1,35]. The simulation model accounted for cell culture geometry and varying intracellular ^{10}B concentrations to calculate the total absorbed dose (Gy), factoring in thermal, epithermal, and fast neutron components, as well as gamma contribution.

Statistical Analysis

Data were expressed as mean ± standard deviation (SD). Differences between groups were analyzed using one-way ANOVA followed by Tukey's post-hoc test. A p-value of < 0.05 was considered statistically significant.

Results

Differential Internalization of BCDs Across Tumor Cell Lines

Establishing sufficient intracellular boron concentration is the rate-limiting step for effective BNCT. Our quantitative ICP-MS analysis revealed substantial heterogeneity in the metabolic handling of BCDs across the tested tumor models (Fig. 2 and Table 1).

In sharp contrast (Supplementary Table 1, 50 ppm group), HepG-2 cells exhibited minimal accumulation under identical conditions, reaching only 0.43 ± 0.04 μg B/mL (0.86% efficiency). B16-F10 cells showed moderate uptake, with an intracellular boron concentration of 10.00 ± 0.06 μg B/mL (20.00% efficiency) following 24 hours of incubation with 50 μg B/mL BCDs. Comparing the extremes, B16-F10 cells showed moderate uptake. Comparing the extremes, U87-MG cells accumulated approximately 43-fold more boron than HepG-2 cells (18.50 / 0.43 ≈ 43). This striking metabolic divergence fundamentally segments the cell lines into "BCDs-sensitive" and "BCDs-resistant" populations prior to any irradiation event.

Cytotoxicity and Identification of a Therapeutic Threshold Control

We break down the scenario and calculations provided. ^{10}B concentration and Tumor Cell Mass: (1) Each tumor cell is assumed to contain about 10^9 ^{10}B atoms. The irradiation parameters are shown in Supplementary Table 2 and 3. Neutron flux and irradiation time combine to produce a neutron fluence of 6.16×10^{11} n/cm^2. The reaction cross-section for ^{10}B is 3835 times 10^{-24} cm^2.

The detailed calculations were as follow:

Number of capture reactions per cell is $\lambda = N_B \times \sigma_B \times \Phi = 2.36$, where $N_B = 10^9$ is number of boron atoms per cell, $\sigma_B = 3835$ b is a cross-section of neutron capture by boron and $\Phi = 6.16 \times 10^{11}$ n/cm^2 is neutron flux.

This matches the provided information that 2.36 capture reactions occur per cell on average. Each capture reaction kills 60% of the affected cell. For 2.36 reactions per cell, the survival rate is given by: $S = S_2 \times P_2 + S_3 \times P_3$, where $S_2 = (1-k)^2$, $S_3 = (1-k)^3$, $P_2 = 0.64$, $P_3 = 0.36$ and $k = 0.6$ (kill rate)[36].

Survival Rate Calculation: S = 12.5%. This aligns with the provided survival rate of 11.50%. The detailed calculations confirm the given values and assumptions. The $^{10}B(n, \alpha)^7Li$ reaction is effective in reducing the survival rate of tumor cells to 11.50% under the described conditions, indicating a promising potential for BNCT in treating tumors with adequate boron delivery and neutron irradiation.

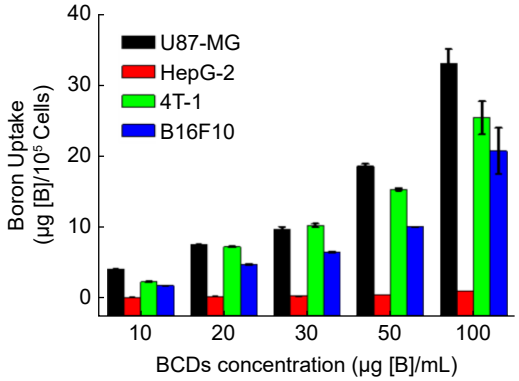

Fig. 2. The boron uptake in different tumor cell lines with boron-containing carbon dots after 24 h incubation.
U87-MG and 4T-1 cells demonstrated robust uptake capabilities (Supplementary Table 1). Upon incubation with an initial BCD concentration of 50 μg B/mL (24 hours post-incubation), U87-MG cells achieved an intracellular concentration of 18.50 ± 0.35 μg B/mL (37.00% internalization efficiency), and 4T-1 cells achieved 15.25 ± 0.18 mg B/mL (30.50% efficiency). This translates to an internalization efficiency of ~ 37%, suggesting that these aggressive tumor phenotypes readily exploit receptor-mediated pathways to internalize these nanoscale entities.

Table 1. The internalization efficiency varies among different tumor cell lines with 50 μg [B]/mL boron-containing carbon dots after 24 h incubation.

Tumor Cell Line	Cancer Type	Intracellular Boron Concentration (μg B/mL) ± SD	Internalization Efficiency (%) ± SD
U87-MG	Glioblastoma	18.50 ± 0.35	37.00 ± 0.70
4T-1	Breast Cancer	15.25 ± 0.18	30.50 ± 0.36
B16-F10	Melanoma	10.00 ± 0.06	20.00 ± 0.12
HepG-2	Hepatocellular	0.43 ± 0.04	0.86 ± 0.08

Dose-dependent BNCT efficacy of BCDs in different tumor cell lines

The binary nature of BNCT was confirmed by control experiments showing negligible toxicity from neutrons alone or BCDs alone at tested doses (Supplementary Figure S1 and Figure S2), confirming that therapeutic efficacy relies solely on the in situ nuclear capture reaction. Among them, B16F10 inevitably produces melanin, which interferes with CCK-8 assay accuracy (resulting in measurement error); In addition, it is also possible that the low sensitivity of B16-F10 to BNCT is mainly due to the low internalization of BCD (24 hours after irradiation, the concentration was 10 mg/mL, Table 1). Therefore, B16F10 cell line was not included in the experimental group.

Following neutron irradiation, cell viability data closely mirrored the uptake profiles. U87-MG and 4T-1 cells experienced profound, dose-dependent cytotoxicity. Crucially, integrating the uptake quantification with viability assays revealed a distinct bio-physical threshold for therapeutic onset. A steep inflection point in the cell survival curve was only observed once intracellular boron concentration breached approximately 20 μg

B/mL, coupled with adequate neutron fluence.

The combination of BCDs and neutron irradiation resulted in significant, dose-dependent cytotoxicity in sensitive cell lines. Consistent with the uptake data, U87-MG and 4T-1 cells exhibited high sensitivity to BNCT. Cell viability decreased significantly as both the BCD concentration and neutron fluence increased (Fig. 3).

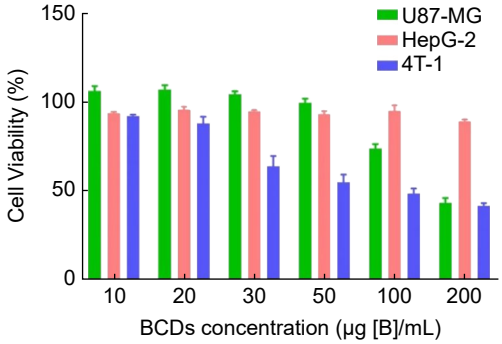

Fig. 3. Biocompatibility Assessment: Cytotoxicity of BCDs Alone Without Neutron Irradiation.
Cell viability of U87-MG (A), 4T-1 (B) and HepG-2 (C) cells incubated with varying concentrations of BCDs ranging from 0 to 200 μg B/mL for 8, 12, and 24 hours in the absence of neutron exposure. The results indicate excellent biocompatibility of BCDs alone at the tested therapeutic concentrations.

U87-MG, 4T-1, and HepG-2 cells exhibited different responses to the combination of boron-containing carbon dots and neutron irradiation. Without boron drugs, neutron irradiation alone would not cause damage to various tumor cells (Supplementary Figure S2). The neutron irradiation alone did not significantly affect tumor cell viability, highlighting the necessity of boron agents for effective therapy. This observation emphasizes the unique synergy between ^{10}B drugs and neutron irradiation. Enhanced therapeutic effects were observed across all cell types when boron-containing carbon dots treatment was combined with neutron irradiation. As the neutron irradiation dose increased, the reduction in tumor cell viability also increased (Fig. 4). In U87-MG cells, cell viability significantly decreased with higher doses of both boron-containing carbon dots and neutron irradiation ($P < 0.01$), demonstrating the potential of boron-containing carbon dots in enhancing BNCT effectiveness. In 4T-1 cells, a noticeable decrease in cell viability occurred at BCDs concentrations ≥ 20 μg B/mL ($P < 0.05$), with an increased sensitivity to higher neutron irradiation doses, indicating a favorable response to BNCT treatment. For U87-MG cells, there was no significant decrease in cell viability at BCD concentrations of 20 ppm and 30 ppm. This was attributed to the fact that at these external concentrations, the boron concentration within the cells had not reached the therapeutic threshold (20 μg B/mL) or the cells had a certain DNA repair capability. HepG-2 cells, due to their innate inability to internalize BCDs, never approached this critical threshold and consequently remained largely viable even at the highest external drug dosages. This resistance in HepG-2 serves as a crucial negative control, demonstrating that high extracellular concentration of boron is therapeutically irrelevant without successful transmembrane delivery.

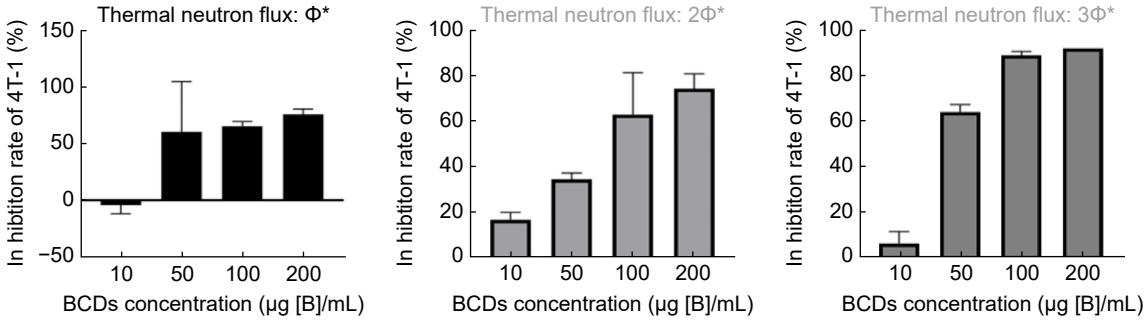

Fig. 4. Control experiment: Effect of neutron irradiation alone on tumor cell viability ($1\Phi^* = 1.54 \times 10^{11}$ n/cm^2).
Viability of different tumor cell lines exposed to thermal neutron irradiation for varying durations without prior BCD incubation. No significant decrease in cell viability was observed compared to non-irradiated controls, confirming the binary nature of BNCT and the lack of toxicity from the neutron beam alone.

Integrating uptake data with viability results revealed a critical therapeutic threshold. A significant inflection points in tumor cell killing was observed only when the intracellular accumulation of BCDs exceeded approximately 20 μg B/mL combined with sufficient neutron irradiation. HepG-2 cells, failing to reach this critical threshold due to poor uptake efficiency, remained largely resistant to the treatment even at high initial drug dosages. Theoretical calculations based on nuclear cross-sections confirm that achieving approximately 10^9 ^{10}B atoms per cell (corresponding to the high uptake observed) is necessary to induce sufficient capture reactions (avg. ~ 2.36 per cell) to reduce survival rates significantly (~ 11.5%).

Micro-dosimetry Analysis

To validate that the observed cytotoxicity was due to the boron capture reaction, Monte Carlo simulations were employed to calculate the total absorbed radiation dose. As shown in Table 2 and Table 3, the total dose delivered to the cells is highly sensitive to the presence of ^{10}B. Under fixed neutron flux conditions (6.16×10^{11} n/cm^2), increasing the boron concentration from baseline (0 ppm) to 13 ppm results in a greater than three-fold increase in total absorbed dose (from 6.91 Gy to 23.50 Gy). This dosimetric data confirms the synergistic mechanism and the necessity of high intracellular boron for effective therapy.

Schematic representation of the cell culture dish setup used in Monte Carlo (PHITS code) simulations to calculate absorbed radiation doses based on cell monolayer geometry and medium composition[1]. Resistance seen in HepG-2 cells without irradiation underscores the necessity of neutron activation for optimal BNCT outcomes. Selectivity and safety: BCDs demonstrated preferential accumulation in tumor cells, with minimal effects on

Table 2. Monte Carlo Simulation of Total Absorbed Dose in BNCT based on Boron Concentration.

Boron Concentration	Simulation Output (eV/g)	B Dose (× 10^{-3} Gy)	The Total Absorbed Dose (× 10^{-2} Gy)				
			1Φ*	2Φ*	3Φ*	4Φ*	SD
0 ppm	5.28	0	1.73	3.46	5.18	6.91	±0.7%
0.65 ppm	5.87	1.95	1.92	3.85	5.77	7.69	±0.6%
1.3 ppm	6.51	4.04	2.13	4.26	6.39	8.52	±0.6%
2.6 ppm	7.78	8.21	2.55	5.10	7.65	10.20	±0.5%
13 ppm	18.00	41.6	5.89	11.8	17.70	23.5	±0.3%

Note: Simulation parameters: 6.5 cm Radial plane beam, fixed thermal neutron flux; $1\Phi^* = 1.54 \times 10^{11}$ n/cm^2.

Table 3. Simulation in 2 cm PE moderated plate.

Thermal Neutrons (<0.5 eV)	Epithermal Neutrons (0.5 eV to 10 keV)	Fast Neutrons (>10 keV)
34.60%	57.20%	8.24%

healthy tissues, aligning with the therapeutic goal of BNCT.

The challenges in evaluating BNCT efficacy in cell experiments are discussed in detail, such as cell state (suspension or adherence), the effect of medium change on boron drug uptake, and the possible "false optimism" results caused by experimental design. This in-depth experimental reflection sheds new light on the reliability of BNCT studies. In analyzing the results, there is less discussion of the advantages and disadvantages of boron-containing carbon dots compared with other boron delivery vectors, such as boron tyrosine or boron phthalocyanine. If the results of this study can be systematically compared with existing technologies, its innovation and application value will be more prominent.

The empirically observed high kill rates in U87-MG cells at concentrations ≥ 18.50 μg B/mL align well with these theoretical predictions.

Discussion

This study provides a comprehensive *in vitro* evaluation of BCDs as radiosensitizers for BNCT, highlighting the critical dependency of therapeutic outcome on cellular metabolic profiles. The distinct variation in boron uptake efficiency - particularly the markedly lower accumulation in HepG-2 cells compared to U87-MG and 4T-1 suggests that BCD internalization pathways are cell-type dependent.

The profound resistance of HepG-2 liver cancer cells compared to the highly sensitive glioblastoma and breast cancer models is consistent with previous reports indicating that HepG-2 cells exhibit poor accumulation of boron-containing nanomaterials due to enhanced xenobiotic clearance mechanisms[11]. We hypothesize this is not merely a difference in passive diffusion but reflective of distinct cell biology characteristics.

Conversely, HepG-2 cells, despite being malignant, retain functional characteristics of hepatocytes, which are the body's primary detoxification units. They possess sophisticated mechanisms to recognize and eliminate xenobiotics. The failure of BCDs to accumulate in HepG-2 is likely due to a combination of (1) reduced basal endocytic rates for nanoparticles of this specific size/charge profile, and significantly, (2) active efflux by multidrug resistance proteins (e.g., P-glycoprotein or MRPs), which are frequently overexpressed in hepatocellular carcinoma. This suggests that for liver cancer applications, BCDs may require surface modification with active targeting ligands (e.g., galactosamine) to bypass these specific resistance mechanisms.

Identifying the 20 μg B/mL intracellular threshold is clinically relevant. This threshold is consistent with earlier publications reporting that effective BNCT requires intracellular boron concentrations of 10–30 μg B/mL. Similar to our findings, Nomoto et al. (2020) demonstrated that poly (vinyl alcohol)-modified boron agents require ~ 20 μg B/mL intracellular concentration to achieve significant tumor cell killing. A key difference between our study and previous work is the broad-spectrum applicability of BCDs across multiple tumor types (U87-MG, 4T-1, B16-F10), whereas most prior studies focused on single tumor models. In BNCT, the therapeutic effect is not linear; it is a threshold phenomenon. The generated α-particles and ^{7}Li nuclei have an ultrashort range (<10 μm). If boron concentration is too sparse, the probability of a particle track traversing the nucleus and causing lethal DNA double-strand breaks drops precipitously. Under standard accelerator neutron flux conditions, the 20 μg B/mL threshold represents the specific boron density required to transition from sublethal cellular damage, which cancer cells can repair, to overwhelming lethal damage. Compared with other boron delivery vectors (e.g., boron tyrosine, boron phthalocyanine), BCDs exhibit several advantages: (1) higher biocompatibility with negligible intrinsic toxicity, (2) fluorescence properties for real-time tracking, and (3) efficient penetration of biological barriers (e.g., blood-brain barrier). However, BCDs also have limitations, such as lower boron loading capacity compared to boron-rich MOFs. Future optimization of BCD synthesis could enhance boron content while maintaining biocompatibility.

Limitations and Future Directions While this in vitro study provides crucial mechanistic insights, it lacks the complex physiological barriers of an in vivo environment, such as blood flow dynamics, the reticuloendothelial system (RES) clearance, and the dense tumor stroma, which will significantly influence BCD biodistribution. Future studies must transition these findings to orthotopic animal models to validate if the metabolic differences observed here translate to tissue-level accumulation differences. Furthermore, delineating the precise molecular endocyt-

ic pathway of BCDs remains a key objective for optimizing their design.

Conclusion

This study validates Boron-containing carbon dots (BCDs) as an effective, biocompatible nanoscale delivery system for BNCT, demonstrating significant therapeutic synergy when combined with thermal neutron irradiation. We established that efficacy is highly dependent on tumor cell type, driven primarily by differential uptake capacities. U87-MG (glioblastoma) and 4T-1 (breast cancer) models showed high sensitivity, while HepG-2 (liver cancer) exhibited resistance linked to poor BCD retention. Crucially, we identified an intracellular concentration threshold of approximately 20 μg B/mL requisite for significant therapeutic outcomes under standard neutron fluence. These findings underscore the potential of BCDs as a broad-spectrum radiosensitizer for solid tumors and highlight the necessity of personalized dosimetry based on tumor metabolic characteristics in future clinical translation attempts.

Abbreviations

^{10}B, Boron-10; 7Li, Lithium-7; ANOVA, Analysis of Variance; BCDs, Boron containing Carbon Dots; BNCT, Boron Neutron Capture Therapy; CCK-8, Cell Counting Kit-8; CSNS, China Spallation Neutron Source; DMEM, Dulbecco's Modified Eagle Medium; DNA, Deoxyribonucleic Acid; eV, Electron Volt; FBS, Fetal Bovine Serum; Gy, Gray; ICP-MS, Inductively Coupled Plasma Mass Spectrometry; LET, Linear Energy Transfer; MOFs, Metal-Organic Frameworks; MRPs, Multidrug Resistance-associated Proteins; OD, Optical Density; PBS, Phosphate Buffered Saline; P-gp, P-glycoprotein; PHITS, Particle and Heavy Ion Transport code System; PMMA, Polymethyl Methacrylate; ppm, parts permillion; RES, Reticuloendothelial System; RPMI 1640, Roswell Park Memorial Institute 1640 Medium; SD, Standard Deviation.

Ethical approval and consent to participate

All procedures involving animals and tumor models were conducted according to Peking University Third Hospital's ethical guidelines for laboratory animal care and use. Approval was granted by the Laboratory Animal Ethics Committee of Peking University Third Hospital of Clinical Medicine (No.SA2024421).

Conflict of Interests

The authors declare no conflict of interest.

Funding

This project was supported by the National Key R&D Program of China (No. 2022YFA1207300 and 2021YFA1201204), the National Natural Science Foundation of China Project (22576010), the directional institutionalized scientific research platform relying on Beijing Synchrotron Radiation Facility (BSRF) of Chinese Academy of Sciences and Guangdong Basic and Applied Basic Research Foundation (2021B1515120037 and 2021B1515140042).

Authors' contributions

HYH: data curation, investigation, methodology and writing – original draft; ZJW: conceptualization, methodology, and writing – original draft; MXY: formal analysis; BBP: validation; SKB: visualization; WHG: resources and project administration; WHZ: resources and formal analysis; GMX: writing – review & editing, funding acquisition, and project administration; and JL: conceptualization, funding acquisition, supervision, and writing – review & editing.

References

[1] Wang Z, Lei R, Zhang Z, et al. Boron-Containing MOF Nanoparticles with Stable Metabolism in U87-MG Cells Combining Microdosimetry to Evaluate Relative Biological Effectiveness of Boron Neutron Capture Therapy. ACS Appl Mater Interfaces, 2024, 16: 3232-3242.

[2] Tang H, Wang Z, Hao H, et al. Boron-Containing Mesoporous Silica Nanoparticles with Effective Delivery and Targeting of Liver Cancer Cells for Boron Neutron Capture Therapy. ACS Appl Mater Interfaces, 2024, 16: 22934-22945.

[3] Luo X, Wang Z, Yang M, et al. Intratumoral Delivery of High Boron-Containing Carbon Quantum Dots for Enhanced Boron Neutron Capture Therapy. ACS Appl Bio Mater, 2025, 8: 5138-5146.

[4] Soloway AH, Barth RF, Carpenter DE. Advances in Neutron Capture Therapy. Springer: New York, USA, 1993.

[5] Sauerwein WAG, Wittig A, Moss RL, et al. Neutron Capture Therapy: Principles and Applications. Springer: Berlin, Germany, 2012.

[6] Lv L, Zhang J, Wang Y, et al. Boron Neutron Capture Therapy-Derived Extracellular Vesicles via DNA Accumulation Boost Antitumor Dendritic Cell Vaccine Efficacy. Adv Sci, 2024, 11: 2405158.

[7] Li J, Chen Z, Wang Z, et al. ^{10}Boron-doped carbon nanoparticles as delivery platforms for boron neutron capture therapy and photothermal therapy. Biomater Sci, 2025, 13: 3280-3297.

[8] Zhang Y, Kang HG, Xu HZ, et al. Tumor Eradication by Boron Neutron Capture Therapy with ^{10}B-enriched Hexagonal Boron Nitride Nanoparticles Grafted with Poly(Glycerol). Adv Mater, 2023, 35: 2301479.

[9] Fujimura A, Yasui S, Igawa K, et al. In Vitro Studies to Define the Cell-Surface and Intracellular Targets of Polyarginine-Conjugated Sodium Borocaptate as a Potential Delivery Agent for Boron Neutron Capture Therapy. Cells, 2020, 9: 2149.

[10] Hosmane NS, Maguire JA, Zhu Y, et al. Boron and Gadolinium Neutron Capture Therapy for Cancer Treatment. World Scientific: Singapore, 2011.

[11] Wang Z, Chen Z, Zhang Z, et al. Multifunctional high boron content MOFs nano-co-crystals for precise boron neutron capture therapy for brain glioma in situ. Nano Today, 2022, 45: 101558.

[12] Hosmane NS. Boron Science: New Technologies and Applications. CRC Press: Boca Raton, USA, 2012.

[13] Itas YS, Suleiman AB, Ndikilar CE, et al. First-Principle Studies of the Structural, Electronic, and Optical Properties of Double-Walled

Carbon Boron Nitride Nanostructures Heterosystem under Various Interwall Distances. J Chem, 2023, 2023: 4574604.

[14] Lv L, Liu Q, Su W, et al. Precise delivery of 10^B at cellular resolution in vivo enhances boron neutron capture therapy effect. Nano Today, 2025, 64: 102773.

[15] Dai LQ, Wang T, Zhou SM, et al. Boronophenylalanine-containing polydopamine nanoparticles for enhanced combined boron neutron capture therapy and photothermal therapy for melanoma treatment. Adv Funct Mater, 2024, 34.

[16] Ali F, Hosmane NS, Zhu Y. Boron Chemistry for Medical Applications. Molecules, 2020, 25: 828.

[17] Liu Q, Lv L, Li H, et al. Microneedle-adapted PAMAM-BSH delivery facilitates spatiotemporal matching for melanoma boron neutron capture therapy. J Control Release, 2025, 384: 113863.

[18] Dai LQ, Liu J, Zhao XS, et al. BPA-containing polydopamine nanoparticles for boron neutron capture therapy in a U87 glioma orthotopic model. Adv Funct Mater, 2023, 33.

[19] Tabbakh F, Hosmane NS. Enhanced biological effectiveness with carbon nanoparticles in proton therapy: a simulation study. Eur Phys J Plus, 2023, 138: 538.

[20] Shuto Y, Nakamura S, Imamichi S, et al. Relative biological effectiveness of an accelerator-based BNCT system coupled to a solid-state lithium target: two different approaches for neutron beams. Appl Radiat Isot, 2025, 222: 111834.

[21] Kuthala N, Shanmugam M, Yao CL, et al. One step synthesis of 10^B-enriched 10^BPO4 nanoparticles for effective boron neutron capture therapeutic treatment of recurrent head-and-neck tumor. Biomaterials, 2022, 290: 121861.

[22] Chen J, Xu M, Li Z, et al. A Bis-Boron Amino Acid for Positron Emission Tomography and Boron Neutron Capture Therapy. Angew Chem Int Edi, 2025, 64: e202413249.

[23] Nomoto T, Inoue Y, Yao Y, et al. Poly (vinyl alcohol) boosting therapeutic potential of p-boronophenylalanine in neutron capture therapy by modulating metabolism. Sci Adv, 2020, 6: eaaz1722.

[24] Chiang CW, Chien YC, Yu WJ, et al. Polymer-Coated Nanoparticles for Therapeutic and Diagnostic Non-10^B Enriched Polymer-Coated Boron Carbon Oxynitride (BCNO) Nanoparticles as Potent BNCT Drug. Nanomaterials, 2021, 11: 2936.

[25] Dai L, Liu J, Yang T, et al. Lipoic acid-boronophenylalanine-derived multifunctional vesicles for cancer chemoradiotherapy. Nat Commun, 2025, 16: 1329.

[26] Icten O, Hosmane NS, Kose DA, et al. Production of Magnetic Nano-bioconjugates via Ball Milling of Commercial Boron Powder with Biomolecules. Z Anorg Allg Chem, 2016, 642: 828-832.

[27] Kashihara T, Nakamura S, Yamazaki N, et al. Boron neutron capture therapy for cutaneous angiosarcoma and malignant melanoma: First in-human phase I clinical trial. Radiother Oncol, 2025, 202.

[28] Tsurubuchi T, Shirakawa M, Kurosawa W, et al. Evaluation of a Novel Boron-Containing α-d-Mannopyranoside for BNCT. Cells, 2020, 9: 1277.

[29] Matović J, Järvinen J, Sokka IK, et al. Towards New Delivery Agents for Boron Neutron Capture Therapy: Synthesis and In Vitro Evaluation of a Set of Fluorinated Carbohydrate Derivatives. Molecules, 2024, 29: 4263.

[30] Icten O, Hosmane NS, Kose DA, et al. Magnetic nanocomposites of boron and vitamin C. New J Chem, 2017, 41: 3646-3652.

[31] Li J, Kong J, Ma S, et al. Exosome-coated 10B carbon dots for precise boron neutron capture therapy in a mouse model of glioma in situ. Adv Funct Mater, 2021, 31: 2100969.

[32] Wang Z, Yang M, Luo X, et al. Revealing a Competitive and Slowed Reaction Mechanism by Using Synchrotron Radiation-Based Semi in Situ Techniques on the Structure Evolution of Functional Carbon Dots. ACS Nano, 2025, 19: 15841-15852.

[33] Tabbakh F, Hosmane NS. Enhancement of Radiation Effectiveness in Proton Therapy: Comparison Between Fusion and Fission Methods and Further Approaches. Sci Rep, 2020, 10: 5466.

[34] Wang Z, Kong J, Chen Z, et al. Human Glioma Nude Mouse Xenograft Model in situ. Dis Res, 2021, 1: 1-5.

[35] Santa Cruz GA. Microdosimetry: Principles and applications. Rep Pract Oncol Radiother, 2016, 21: 135-139.

[36] Weyrather WK, Kraft G. RBE for carbon track-segment irradiation in cell lines of differing repair capacity. Int J Radiat Biol, 1999, 75: 1357-1364.